

# Leaf Area Indices of Forest Canopies from Optical Measurements

AVE KODAR<sup>1</sup>, RIIN KUTSAR<sup>1</sup>, MAIT LANG<sup>2,3</sup>, TÖNU LÜKK<sup>2,3</sup> AND TIIT NILSON<sup>3\*</sup>

<sup>1</sup> Faculty of Science and Technology; Tartu University, Ülikooli 18, 50090 Tartu, Estonia

<sup>2</sup> Institute of Forestry and Rural Engineering, Estonian University of Life Sciences, Kreutzwaldi 1, 51014 Tartu, Estonia

<sup>3</sup> Tartu Observatory, 61602 Tõravere, Tartumaa, Estonia

\* Corresponding author

Kodar, A., Kutsar, R., Lang, M., Lökk, T. and Nilson, T. 2008. Leaf Area Indices of Forest Canopies from Optical Measurements. *Baltic Forestry*, 14 (2): 185–194.

## Abstract

Ground-based estimates of leaf area indices (LAI) of forest canopies and understorey vegetation in Järvselja, Estonia were derived from measurements by the plant canopy analyzers LAI-2000 and hemispherical photographs as well as via allometric relations from traditional forest inventory variables from a forestry database. Regressions of LAI with the SPOT and Landsat satellite image-derived reflectance factors and combined indices were established. The LAI values correlated the best with the reduced simple ratio index defined by the red, near and middle infrared bands. The standard error of the estimate of all regressions between the LAI and satellite image-based variables is about 1.5 units or higher.

**Key words:** Leaf area index, forest, remote sensing

## Introduction

Leaf area index (LAI) was first defined in 1947 as the total one-sided area of photosynthetic tissue per unit ground surface area (Watson 1947). The LAI of vegetation depends on species composition, developmental stage, prevailing site conditions, seasonality, and the management practices (Jonckheere *et al.* 2004). LAI is a key structural characteristic of forest ecosystems because of the role of green leaves in controlling many biological and physical processes in plant canopies. Accurate LAI estimates are required in studies of ecophysiology, atmosphere-ecosystem interactions, and global change (Chen *et al.* 1997).

LAI values can be obtained using direct or indirect ground based methods or from remote sensing products (Jonckheere *et al.* 2004). Among direct LAI measurement methods are harvesting techniques such as destructive sampling and *the model tree method*. Non-harvesting method is using litter traps for deciduous forests during leaf-fall periods in autumns (Chen *et al.* 1997). Direct LAI measurements are the most accurate in principle, but they have the disadvantage of being extremely time-consuming. Time-consuming makes large-scale implementation of direct measurements only marginally feasible; however, direct methods can be considered important as calibration methods (Jonckheere *et al.* 2004).

Indirect methods, in which leaf area is inferred from observations of another variable, are generally faster, amendable to automation and thereby allow for a larger spatial sample to be obtained (Jonckheere *et al.* 2004). Allometric relationships to estimate LAI can be obtained by destructively sampling trees and determining the biomass and area of various components, or they can be obtained from other studies (Marklund 1988, Chen *et al.* 1997).

Indirect non-contact LAI measurement methods (optical methods) are based on the measurement of light transmission through canopies. There are two main categories of instruments developed to indirectly assess LAI of plant canopies. First group contains instruments that are based on *gap fraction* analysis: the DEMON (CSIRO, Canberra, Australia), the Sunfleck Ceptometer (Decagon Devices Inc., Pullman, WA, USA), the LAI-2000 Plant Canopy Analyzer (Licor Inc., Nebraska) and the Multiband Vegetation Imager (MVI) developed by Kucharik and Norman (1996) and hemispherical canopy photography (Evans and Coombe 1959, Anderson 1964). Second group contains instruments that are based on *gap size distribution*: the Tracing Radiation and Architecture of Canopies (TRAC) (3<sup>rd</sup> Wave Engineering, Ontario, Canada) and hemispherical canopy photography.

The monitoring of Earth's biosphere is one of the most important objectives of modern remote sensing.

Global assessment of different biosphere parameters is a target for scanner systems like MODIS, MERIS, MISR, SEAWIFS, VEGETATION *etc.* The coarse resolution MODIS vegetation products are being used by scientists from a variety of disciplines, including oceanography, biology, and atmospheric science (<http://modis.gsfc.nasa.gov/>).

To test the quality of biophysical products there are many international projects, among others the VALERI (Validation of Land European Remote sensing Instruments) (<http://www.avignon.inra.fr/valeri/>) project. One of the objectives of the VALERI project is to provide high spatial resolution maps of biophysical variables (LAI, fAPAR (fraction of absorbed photosynthetically active radiation)) estimated from ground measurements to validate products derived from satellite observations.

**Spectral Vegetation Indices**

Remote sensing provides the only feasible way for the estimation or monitoring of LAI over large territories. Models developed for application of remotely sensed optical data rely on physically based relationships between the LAI and canopy spectral reflectances, typically expressed in the form of spectral vegetation indices (SVI). SVIs in use for the estimation of canopy parameters attempt to enhance the spectral contribution of vegetation while minimizing those from the background (Stenberg *et al.* 2003). For estimation of green vegetation LAI, SVIs based on the ratio or some combination of red (RED) and near-infrared (NIR) reflectance, such as the simple ratio (SR) or the normalized difference vegetation index (NDVI), are commonly used. The indices are preferably calculated from top-of-canopy level reflectance (R) values in the NIR and RED bands.

$$SR = R_{NIR} / R_{RED}, \tag{1}$$

$$NDVI = (R_{NIR} - R_{RED}) / (R_{NIR} + R_{RED}). \tag{2}$$

However, there is often considerable scatter evident in the relationship as influenced by the type and amount of forest understorey or background (shrubs, grasses, moss, lichen or soil) observed by the sensor. The amount of background observed through a forest canopy is mainly determined by canopy cover. To compensate for differences in canopy cover and background reflectance, studies have used additional short-wave infrared (SWIR) reflectance to derive an index termed the reduced simple ratio (RSR):

$$RSR = R_{NIR} / R_{RED} [1 - (R_{SWIR} - R_{SWIRmin}) / (R_{SWIRmax} - R_{SWIRmin})], \tag{3}$$

where  $R_{SWIRmax}$  and  $R_{SWIRmin}$  were represented by the largest and smallest reflectance values in the SWIR band (Brown *et al.* 2000).

Alternatively, the SWIR band has been included in another simple ratio index ISR which was demonstrated by Ahren *et al.* (1991) and Fernandes *et al.* (2004) to be in good correlation with LAI:

$$ISR = R_{NIR} / R_{SWIR} \tag{4}$$

In this paper we used different methods to estimate LAI for the forests in the VALERI test site in Järvelja, Estonia. LAI was derived from 1) optical ground measurements in summers 2001- 2005 and 2) forestry database. The aim was to assess the issues related to the methods, to test the links of LAI to the satellite image-derived spectral indices and their applicability to estimate LAI via remote sensing methods. A further goal is the extension of the methodology to larger areas, such as the whole Estonia and Baltic region.

**Materials and methods**

**Site Description**

The study area is located on the territory of the Järvelja Training and Experimental Forest District belonging to the Estonian University of Life Sciences in south-east Estonia, near Lake Peipsi. The test site for the VALERI project where the ground campaigns were carried out is a flat 3x3-km<sup>2</sup> square, centered at the geographical coordinates 58°15'N and 27°28'E. This region is mostly covered by a sub-boreal pure and mixed forest, including both conifer and broad-leaved deciduous trees. The dominating forest types are birch (*Betula pendula*, *B. pubescens*) forests growing on the *Filipendula* site type and (drained) eutrophic swamps, Norway spruce forests growing on *Oxalis-myrtillus*, *Filipendula* site type and drained *Oxalis* swamps, black alder (*Alnus glutinosa*) forests growing on *Filipendula* and drained swamps and Scots pine forests growing on *Oxalis-myrtillus*, *Oxalis-Rhodococcum* and drained *Oxalis* swamps. Forests are managed according to regular practice in Estonia and nearly 14% of the area of the VALERI test site are regenerating stands where tree layer is sparse or trees are small. Agricultural fields are almost missing within the test site but few unmanaged open areas are present. Last regular forest inventory in Järvelja Training and Experimental Forest District was carried out in 2001. An outcome of the inventory was the database with descriptive characteristics of forest stands and a digital map of stand borders.

**Subsets of forest data for the analysis**

In addition to ground-based sample plot data, three larger subsets of stands were chosen for the analysis.

From the forestry database by means of SQL-queries 75 spruce, 56 birch and 61 pine dominated stands were selected. In addition to selecting stands with fixed main species, the following conditions superimposed in the queries were: the main tree species percentage >75%, stand size >1ha (spruce), >2ha (pine), >3ha (birch). The stand average reflectance factors and vegetation indices for the queried stands were extracted from the satellite images by the PixelWin program (Lükk 1999) with the help of digital map of stand borders over Järvselja. We studied the relations between the allometric tree-layer LAI ( $LAI_{trces}$ ) and total LAI ( $LAI_{total}$ ) with the image-derived reflectance factors and indices SR, NDVI, ISR and RSR. The statistical analysis was performed using the STATISTICA (vers5.0) programme.

#### *Leaf area index measurements*

Ground measurements by means of plant canopy analyzers (PCA) were made on 50-70 sample plots on summers 2001, 2002, 2003 and 2005. Plot centers were located at least 50m from the stand edge, their locations measured by tape from stand edge and marked. The coordinates of plot centers were measured on the digital stand map and later checked by means of a GPS instrument. The uncertainty of plot center location was less than half of the SPOT pixel – 10m. Two types of PCA were used, LAI-2000 and hemispheric canopy photography. Sample plots were chosen to be representative for the whole 3x3 km area according to the unsupervised classification of Landsat ETM+ image from 10 July 1999. The same plots were mostly re-measured each year. A general description of the selected stands is given in Table 1. According to the methodology accepted in the VALERI project (<http://www.avignon.inra.fr/valeri/>), LAI-2000 measurements were made at points displaced by 4m, 8m and 12m from the centre of the plot in each geographic direction, in

**Table 1.** A short summary of forestry data of the stands sampled in the course of ground-based PCA campaign in Järvselja

| Dominating species | Age, years | Orlov (1929) site index | Basal area, m <sup>2</sup> /ha |
|--------------------|------------|-------------------------|--------------------------------|
| Birch              | 5-65       | 1-3                     | 4.3-31.8                       |
| Black alder        | 5-65       | 1a-3                    | 0.2-29.4                       |
| Pine               | 65-175     | 1a-2                    | 26-31.5                        |
| Spruce             | 20-68      | 1-4                     | 8.2-28.3                       |
| Mixed              | 17-75      | 1-5                     | 6.2-29                         |
| Clear cut          | 0-8*       | 1-5                     | 0                              |

\*Time (in 2005) in years from clear cutting

the fixed sequence N-S-E-W. At each point, 4 records at the ground level and 4 records at the breast-height level (1.3 m) were collected within the distance of 1m. In total, on a sample plot 96 LAI-2000 readings were taken ( $3 \times 4 \times 4 \times 2 = 96$ ). The sensor was partly screened with the 180° mask to avoid the influence of the operator, and was always oriented with the sun in the back of the operator to avoid the influence of direct solar radiation.

The reference measurements (above canopy) were acquired in an automatic procedure (each 30s) by another LAI-2000 instrument displayed in an open area (clearing) close to the sample plots. The reference sensor in the open was operated with the 180° mask, too. The LAI-2000 analyzers were regularly inter-calibrated (4-6 times a day) in an open place, and the calibration coefficients were taken into account when calculating the gap fractions.

#### *Hemispherical canopy photography*

During the campaign, hemispherical photographs were recorded with Nikon CoolPix 4500 digital camera supplied with fisheye converter (FC-E8). Images were recorded at each LAI-2000 measuring location at approximately breast height level (1.3m), camera optical axis pointed to zenith and camera oriented in N-S direction. The images were stored into JPEG format using 1600x1200 pixels size. Camera was operated in the aperture priority mode. Point light measurement mode was used with exposure locked at slightly below the sky-canopy border which seemed to attain the best exposure for the entire canopy. To avoid scene underexposure and local sensor saturation by directly looking at the Sun, whenever it was possible recording location was shifted (+/- 1m) so that the Sun was blocked by a near-by tree trunk.

The processing of hemispheric images was done by means of the CAN\_EYE software ([http://www.avignon.inra.fr/can\\_eye/](http://www.avignon.inra.fr/can_eye/)). From the program output the average fraction of canopy gaps as the function of view zenith angle with the angular step of 2.5° was used. To reduce the subjectivity of processing, three independent operators analyzed the whole set of images and later the averaged gap fraction over all operators was used for the subsequent analysis. As the output from both PCA methods, the angular distribution of the canopy gap fraction was used to derive the LAI. The angular distribution of gap fraction was averaged over all photos taken on the plot (see an example on Figure 1). Similarly, the average gap fraction angular distribution for a plot was obtained from the LAI-2000 measurements. Finally, the average angular distribution of gaps obtained by the two methods was used to estimate LAI of the plot.

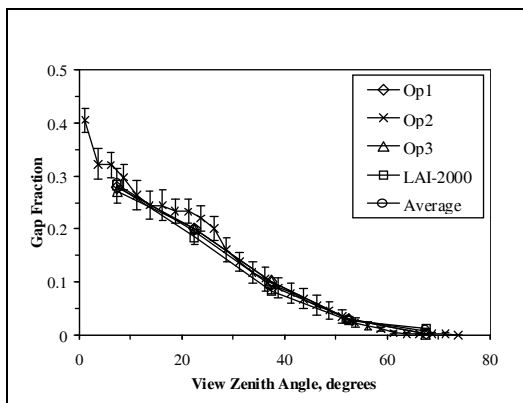


**Figure 1.** An example of the measured canopy gap fraction as a function of view zenith angle determined from hemispheric photos by three operators (Op1, Op2, Op3), by means of LAI-2000 PCA and as the average of both methods

**Derivation of LAI from gap fraction data**

The default procedures in the LAI-2000 PCA and CAN\_EYE for processing the hemispheric photos calculate the so-called effective plant area index. The latter includes the LAI of the tree layer, but also the woody part and is biased due to foliage clumping. In this study, our aim was to estimate the ‘true’ green LAI.

The average gap fraction data for a sample plot was inverted for LAI using the theoretical gap fraction formulas from Nilson (1999) and Nilson and Kuusk (2004):

$$LAI = \frac{-2N}{\kappa + \alpha} \int_0^{\pi/2} S(\theta) \ln \left[ 1 - \frac{1 - \exp[(1 - \zeta) \ln a(\theta) / NS(\theta)]}{1 - \zeta} \right] \cos \theta \sin \theta d\theta \quad (5)$$

where  $N$  is the stand density (trees/m<sup>2</sup>),  $\kappa$  - the shoot-level clumping factor,  $\alpha$  - the branch area to leaf area ratio,  $S(\theta)$  - crown envelope projection area (m<sup>2</sup>) on the horizontal plane in the direction with the view zenith angle  $\theta$ ,  $\zeta$  - Fisher’s grouping index of the tree distribution pattern,  $a(\theta)$  – the measured fraction of canopy gaps at the view angle  $\theta$ . To apply Eq. 5, estimates of  $N$ ,  $\kappa$ ,  $\alpha$ , as well as tree crown dimensions (crown radius  $R$  and depth  $L_{CR}$ , tree height  $H$ , breast-height trunk diameter  $D_{1.3}$ ) to calculate the crown projection area should be known. The dimensions, not directly included in the database (crown depth and radius) were calculated via regressions on the measured variables, like  $D_{1.3}$  and  $H$  (see also Lang *et al.* 2007). Two possible crown forms were used, an ellipsoid for deciduous species and a cone on top of a cylinder for conifers. Fisher’s grouping index  $\zeta$  was approximately calculated from the relations

$$c_B = -\ln(1 - C_{CAN}) / C_{CR} \text{ and } c_B = -\ln \bar{i} / (I - \bar{i}), \quad (6)$$

where  $C_{CR}$  is the crown cover (sum of vertical crown projection areas per unit ground area) and  $C_{CAN}$  the canopy cover (sum of vertical crown projection areas per unit ground area, overlapped areas counted only once). Crown cover was estimated by knowing the stand density and (effective) crown radius. Canopy cover estimate was derived from the gap fraction value estimated in the uppermost ring of LAI-2000 instrument and correcting for the transparency of a single crown (Nilson and Kuusk 2004).

In practical calculations, before applying Eq. 5, the role of tree trunks in the measured gap fraction  $a(\theta)$  was eliminated. It was done applying the respective theoretical formulas describing the shadowing role of tree trunks (Nilson and Kuusk 2004) by using the trunk projection areas calculated by knowing the trunk diameter  $D_{1.3}$  and tree height  $H$  together with the species-specific trunk tapering curves by Ozolins (2002).

**Satellite Data**

SPOT 4 HRVIR images over Järvelja from 4 July 2001, 13 July 2002, 26 June 2003 and Landsat 7 ETM+ image of 5 July 2005 were used in the study. All spectral bands of SPOT4 HRVIR were used XS1 (green): 500-590, XS2 (red): 610-680, XS3 (near infrared): 780-890, XS4 (middle infrared): 1580-1750nm while from the Landsat 7 ETM+ image – three bands TM3 (red): 630-690, TM4 (near infrared): 780-900, TM5 (middle infrared): 1550-1750nm. All images were georeferenced into the Lambert-Est 1992 coordinate system using an individual set (from 40 to 50) of control points with residual location error in all cases less than 0.5 map unit size of a pixel. All images were further transformed into the top of canopy reflectance factor units by using the atmospheric correction by the 6S algorithm (Vermote *et al.* 1997). The set of images in use belongs to a larger set of Landsat and SPOT images over Järvelja forming an image series over years 1986-2007. A smoothing of the image calibration coefficients was applied (Nilson *et al.* 2007) to the whole set of images. As a result, reasonably smooth seasonal reflectance course of different types of forest was obtained and the midsummer reflectance factors of the same forest types from different years used in this study became well comparable in their absolute values and spatial variability. In this study, we have focused on LAI distribution during midsummer (July) that should coincide with the maximum photosynthetic capacity of the vegetation being observed.

**Allometric LAI**

Tree-layer leaf area index (LAI<sub>trees</sub>) estimate was added into the forest inventory database. Allometric

regression models from Marklund (1988) were used to estimate foliage dry mass per tree. LAI for the stands was calculated from mass via specific leaf weight (SLW,  $\text{g/m}^2$ ) and number of trees per hectare ( $N$ ). The used SLW values are given in Table 2.

**Table 2.** The species specific SLW values used in the derivation of leaf area from leaf weight data

| Species                                | SLW ( $\text{g m}^{-2}$ ) |
|--|---------------------------|
| <i>Pinus sylvestris</i> <sup>1</sup>   | 167                       |
| <i>Picea abies</i>                     | 151                       |
| <i>Fraxinus excelsior</i> <sup>2</sup> | 83.3                      |
| <i>Populus tremula</i> <sup>2</sup>    | 86.9                      |
| <i>Alnus glutinosa</i> <sup>2</sup>    | 77.5                      |
| other deciduous species <sup>2</sup>   | 75.8                      |

<sup>1</sup> Smolander and Stenberg (1996)

<sup>2</sup> Niinemets and Kull (1994)

Arguments for foliage mass models were forest inventory variables tree height ( $H$ ), tree trunk diameter at breast height ( $D_{1.3}$ ) for conifers and additionally tree crown depth ( $L_{CR}$ ) estimate for deciduous trees calculated as

$$L_{CR} = \ln(0.5525 H/D_{1.3} + \exp(0.7032 \ln(D_{1.3}))). \quad (7)$$

Lang *et al.* (2007) tested several allometric foliage mass models including those of Marklund (1988) and found that the models including  $H$  and  $L_{CR}$  as an argument in addition to the traditional  $D_{1.3}$  can be considered slightly more independent of the growth conditions compared to pure  $D_{1.3}$  based models. By including  $H$  and  $L_{CR}$  the information about crown envelope volume is taken into account which is well related to the foliage density and stand density. Pure  $D_{1.3}$  based models, ignore stand density effects and tend to give wider range for foliage mass estimates on the same dataset.

Ground vegetation LAI was calculated into the database according to the regression equation

$$\text{LAI}_{\text{ground}} = -0.2064 \text{LAI}_{\text{trees}} + 1.609, \quad (8)$$

which is based on our results of LAI-2000 measurements at the breast-height and ground level carried out in Järvelja during the VALERI campaign in 2002.

## Results

### PCA LAI versus allometric LAI

Figure 2 represents the correlation diagram of tree layer LAI estimates as obtained from the ground-based PCA measurements in 2005 and allometric LAI. Since the forestry database is from 2001, the stands where after the year 2001 clear cutting occurred were excluded from the analysis. No systematic differences between deciduous, coniferous and mixed forests could be noticed. Regression between allometric LAI and PCA LAI is quite good ( $r^2=0.59$ , standard error of the estimate (SEE)=0.94). Results of similar quality were obtained when the LAI-2000 PCA data of the 2002 campaign were analyzed and compared with the allometric LAI. This fact gives us an encouragement to use the allometric LAI to establish and test relationships between different satellite image-derived quantities and LAI. In this case the analysis could be performed on considerably larger data sets compared with rather limited amount of sample plots available in ground based PCA measurements.

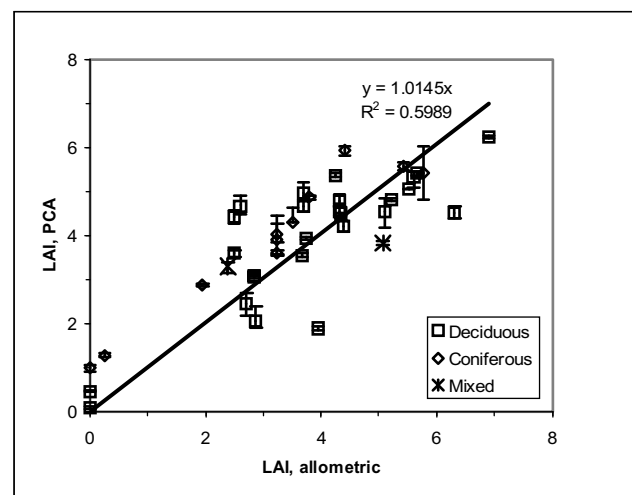


**Figure 2.** Scatterplot of canopy LAI values derived via allometric relations and from PCA measurements (2005). Error bars represent the standard error of the estimate by different PCA

### Allometric LAI versus satellite image derived reflectance

Spectral reflectance factors and vegetation indices were tested for their sensitivity to both the allometric canopy  $\text{LAI}_{\text{trees}}$  and total  $\text{LAI}_{\text{total}}$  (canopy + understory). Since the results were rather similar, in this study we present figures on  $\text{LAI}_{\text{total}}$  only. The reflectance factors in all SPOT 4 HRVIR spectral bands showed a decreasing trend with increasing LAI (Figure 3a-3d) and an increase in all the indices ISR, RSR, SR and NDVI (Figure 3e-3h).

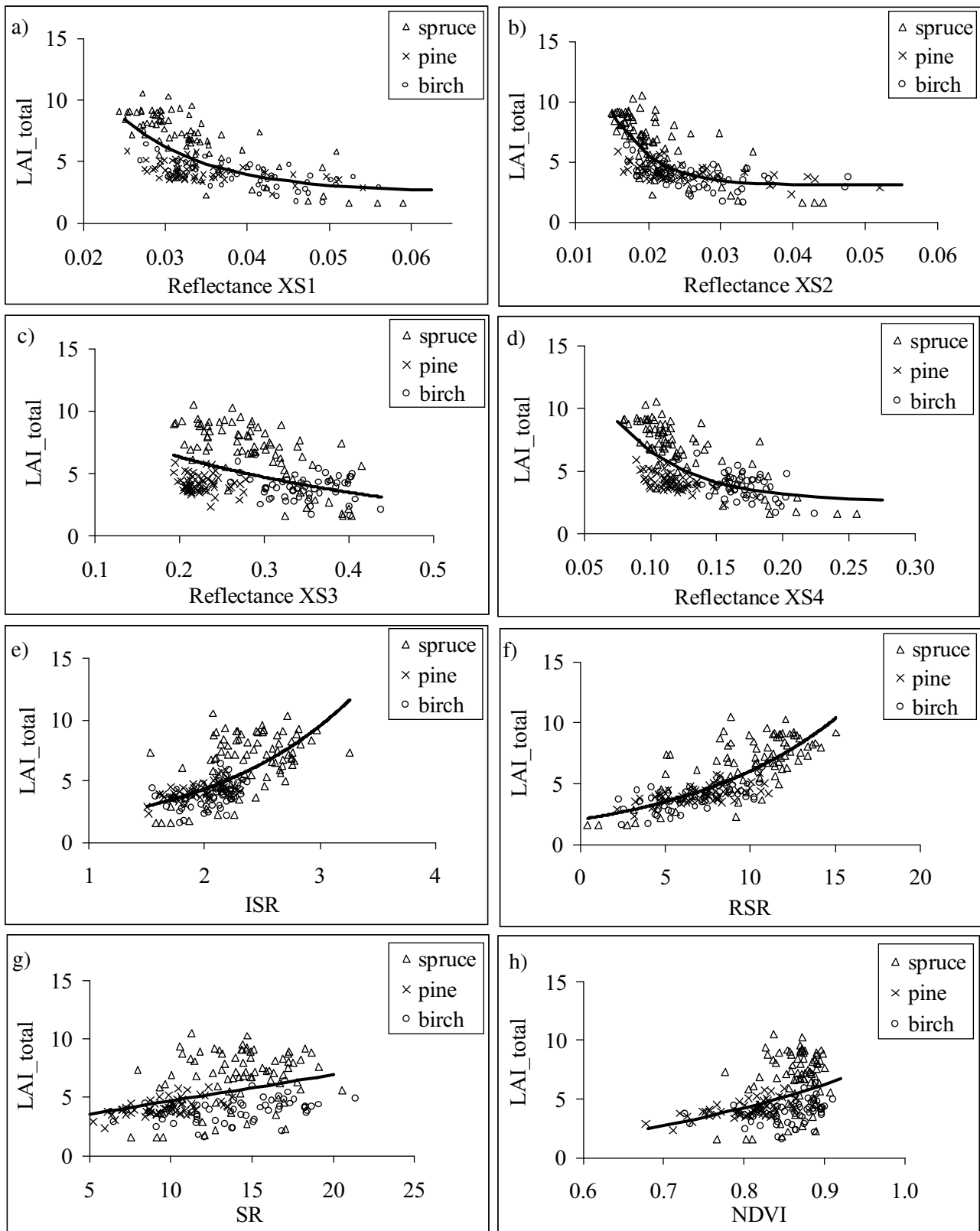


**Figure 3.** Relationship between LAI<sub>total</sub> with SPOT 4 HRVIR reflectance factors in bands 1, 2, 3 and 4 as well as ISR, RSR, SR and NDVI indices for spruce, pine and birch dominated stands in Järvelja. The SPOT image is of 4 July 2001. Bands: XS1 - green (500-590nm); XS2 - red (610-680nm); XS3 - near infrared (780-890nm); XS4 - middle infrared (1580-1750nm)

The relationships between the LAI and reflectance factors  $R_1$ - $R_4$  or indices ISR, RSR are slightly non-linear (Figure 3), an exponential relationship appears to be more appropriate than the linear. The reflectance in the near infrared band (Figure 3c) appears to be relatively insensitive with respect to LAI. Multiple linear and exponential regressions were also applied and the summary results are given in Tables 3 and 4. All the indices had positive correlation with LAI but differed with respect to their predictive power and by the sensitivity to changes in LAI. RSR correlated slightly better with LAI ( $R^2=0.58$ )

than did ISR ( $R^2=0.41$ ) while NDVI had a poor correlation ( $R^2=0.15$ ). According to our data, RSR seems to be the best remote sensing index among single predictors for the LAI. The best regression was obtained when we used reflectances in all spectral bands and also included both indices ( $R^2=0.62$ ,  $SEE=1.27$ ). However, the standard error of the estimate was still quite large. When the similar analysis was performed for the year 2005, weaker correlations were obtained ( $R^2=0.52$ ;  $SEE=1.44$ ), most probably caused by the fact that the database was somewhat out of date by that time.

**Table 3.** Multiple linear regression summary in 2001. Model:  $y=B_0+B_1 x_1+B_2 x_2+\dots$ . B0-intercept, B1-reflectance XS1, B2-reflectance XS2, B3-reflectance XS3, B4-reflectance XS4, B5-RSR, B6-ISR, R<sup>2</sup>- part of variance explained, SEE- standard error of the estimate

| Dependent variable | B0     | B1        | B2       | B3       | B4       | B5     | B6     | R <sup>2</sup> | SEE  |
|--------------------|--------|-----------|----------|----------|----------|--------|--------|----------------|------|
| LAI-total          | 9.537  | -139.086* | 100.719* | 23.193   | -63.058* |        |        | 0.53           | 1.45 |
|                    | -5.370 | -80.934   | 91.105   | -27.924* | 48.096*  | 0.406* | 4.363* | 0.62           | 1.31 |
| LAI-trees          | 9.724  | -174.295* | 127.981* | 28.833   | -77.525* |        |        | 0.54           | 1.73 |
|                    | -7.751 | -101.703  | 115.752  | -30.893* | 52.323*  | 0.492* | 4.996* | 0.63           | 1.57 |

\*significant at 0.05 level

**Table 4.** Exponential regression summary in 2001: model  $y=C+\exp(B_0+B_1*x_1+B_2*x_2 \dots)$ . Coefficients B1-reflectance XS1, B2-reflectance XS2, B3-reflectance XS3, B4-reflectance XS4, B5-RSR, B6-ISR, R<sup>2</sup>- part of variance explained, SEE- standard error of the estimate. Lines represent different combinations of spectral bands and indices used in the regression

| Regression  | C       | B     |         |         |        |         |       |        |      | R <sup>2</sup> | SEE |
|-------------|---------|-------|---------|---------|--------|---------|-------|--------|------|----------------|-----|
| Exponential |         | B0    | B1      | B2      | B3     | B4      | B5    | B6     |      |                |     |
| LAI-total   | 2.523   | 4.212 | -97.715 |         |        |         |       |        | 0.42 | 1.59           |     |
|             | 3.080   | 4.625 |         | -187.18 |        |         |       |        | 0.54 | 1.41           |     |
|             | -45.030 | 3.970 |         |         | -0.194 |         |       |        | 0.09 | 1.99           |     |
|             | 2.562   | 3.341 |         |         |        | -19.182 |       |        | 0.42 | 1.59           |     |
|             | -0.155  | 0.792 |         |         |        |         | 0.102 |        | 0.58 | 1.35           |     |
|             | -18.010 | 2.768 |         |         |        |         |       | 0.172  | 0.41 | 1.59           |     |
|             | 2.792   | 3.844 | -36.099 | -48.066 | 7.136  | -22.199 |       |        | 0.62 | 1.29           |     |
| LAI-trees   | 1.715   | 1.151 | -18.235 | 15.964  | 0.651  | -6.599  | 0.119 | -0.019 | 0.63 | 1.27           |     |
|             | 1.060   | 4.260 | -91.653 |         |        |         |       |        | 0.42 | 1.91           |     |
|             | 1.825   | 4.696 |         | -179.50 |        |         |       |        | 0.54 | 1.71           |     |
|             | -59.190 | 4.204 |         |         | -0.184 |         |       |        | 0.09 | 2.40           |     |
|             | 0.956   | 3.368 |         |         |        | -16.977 |       |        | 0.42 | 1.91           |     |
|             | -2.512  | 1.120 |         |         |        |         | 0.095 |        | 0.59 | 1.61           |     |
|             | -24.670 | 3.005 |         |         |        |         |       | 0.168  | 0.42 | 1.92           |     |
|             | 1.389   | 3.862 | -40.237 | -33.930 | 7.320  | -21.952 |       |        | 0.62 | 1.55           |     |
|             | -0.519  | 1.275 | -17.642 | 18.839  | 0.268  | -4.567  | 0.104 | 0.045  | 0.63 | 1.53           |     |

**PCA LAI versus image derived RSR index**

In Figure 4, the results of ground based LAI measurements made on sample plots in different years are plotted against the RSR index estimated for the same stands from the satellite images of the respective year and a summary of regressions is given in Table 5. For comparison, the regression between the allometric LAI and RSR of the year 2001 is given. This regression shows somewhat higher slope as compared with the PCA LAI regressions. A possible conclusion that could be drawn is that the used allometric relations tend to slightly overestimate LAI, especially in denser forests. As it can be seen, the regressions in different years are somewhat different. The non-linearity of the relation, that was present in Figure 3, is not obvious. When to use regressions from Figure 4 to estimate forest LAI from satellite images, the uncertainty of the estimate remains quite high.

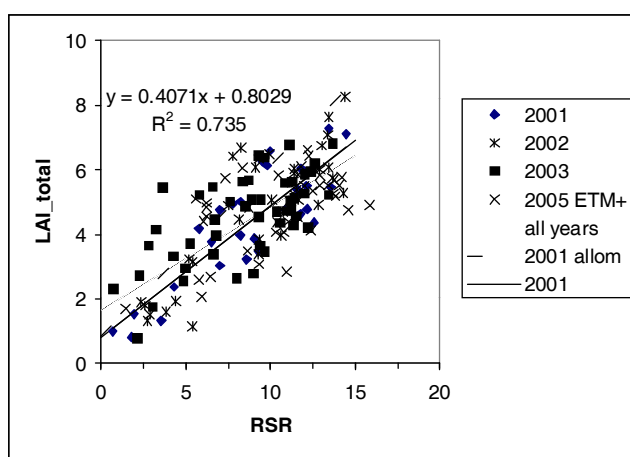


**Figure 4.** Scatterplot between total LAI from ground-based measurements and satellite image-derived RSR index. Different kind of symbols correspond to different year campaigns. The regression equation in the figure is for the 2001 campaign. The dashed line corresponds to the regression line for the 2001 image and LAI<sub>total</sub> as determined via allometric relations

**Table 5.** Linear regression summary of LAI<sub>total</sub> as measured during ground campaigns on the RSR index measured from the satellite images of different years. R<sup>2</sup>- part of variance explained, SEE- standard error of the estimate

| Campaign year   | Slope  | Intercept | R <sup>2</sup> | SEE  |
|-----------------|--------|-----------|----------------|------|
| 2001            | 0.4071 | 0.802     | 0.735          | 0.92 |
| 2002            | 0.4327 | 0.689     | 0.692          | 1.10 |
| 2003            | 0.2765 | 2.171     | 0.498          | 1.00 |
| 2005            | 0.2108 | 2.589     | 0.328          | 0.99 |
| All years       | 0.3195 | 1.647     | 0.531          | 1.06 |
| Allometric 2001 | 0.5274 | 0.856     | 0.567          | 1.62 |

**Discussion and conclusions**

The results obtained mostly confirmed the earlier results in the boreal forests (Chen *et al.* 2002, Stenberg *et al.* 2004, Rossello 2007). Single band reflectances, especially in the green, red and middle infrared regions correlate reasonably well with the forest LAI. RSR index performs somewhat better than the ISR index and considerably better to estimate the LAI than the widely used NDVI. The relation between LAI and RSR index was less sensitive to dominating tree species if compared with the relation between LAI and ISR index. The conclusion was drawn by an analysis of residuals of regressions in Figures 3f and 3e, separately for spruce, pine, and birch dominating stands. The insensitivity of the relation is extremely important if the aim is to apply remote sensing in the LAI estimation.

Although the direct comparison of LAI values as obtained from PCA measurements and allometric relations did not show non-linearity, somewhat non-linear relations were observed between the allometric LAI and the majority of satellite image derived quantities. It is quite possible that the non-linear appearance of the relations is a result of applied allometric equations which overestimate LAI in dense forests.

Parallel use of two kinds of PCA (LAI-2000 and digital hemispheric camera) as well as application of several operators to process hemispheric photos produced more reliable gap fraction estimates. However, the increased reliability was achieved at the expense of more labour power involved.

Although the processing of hemispheric images has considerably improved after appearing new sophisticated packages such as CAN\_EYE, there is still some uncertainty and subjectivity in the estimation of gap fraction from the images. A considerable part of the uncertainty seems to be caused by automatic non-linear gamma-correction of the pixel values in commercial cameras. As suggested by Cescatti (2007), one of the options to reduce these effects is saving the images in the raw image format. Then the linear relations are preserved and the processing of images would be more like it is done in the LAI-2000 instrument. However, processing the hemispherical digital camera raw data needs different approach than it is available in most of the software packages.

A possibility to estimate the true LAI values of forest canopies values by Nilson's algorithm instead of effective LAI determined by default PCA algorithms has its problematic issues, too. First of all, in order to apply the algorithm, a lot of a priori stand structure data is needed. The same variables could well be used to derive an allometric LAI estimate for the stand. So,



the main role of PCA measurements and derivation of the true LAI estimate via Nilson's algorithm would be checking the validity of allometric relations applied. Certainly, there are problems with the applied values of species specific coefficients  $\kappa$ ,  $\alpha$ , SLW and possible dependence of these values on site type and quality. Data quality in the database could be better to apply the allometric relations.

Other methods, such as the derivation of LAI from gap size analysis have been applied (Chen *et al.* 2002). Since the TRAC instrument needs perfect weather conditions, gap size analysis from hemispheric photos seem to be more appropriate. There is a hope that lidar systems would provide new possibilities to LAI estimation. However, lidar measurements are too expensive at the moment to be used as a routine.

Allometric regressions should be tested on extended material; so far the relations ignore seasonality and LAI variability from year to year. More data are needed to check the applicability of remote sensing in forest LAI estimation. To carry out more and wider ground based tests, it is highly recommended to include PCA measurements into the routine forest inventory measurement campaigns.

One of the ideas of careful atmospheric correction of images was to study the possibility to extend the regressions between forest LAI and remotely sensed data from one year to another. A confirmation was obtained that for the well-calibrated images the use of regressions from another years is possible with a marginal decrease in the predictive power of the regression. However, the SEE of all regressions with remotely sensed variables remains quite high, being typically of the order of 1.3-1.5 units of LAI. One has to consider these uncertainty numbers when the regressions are used to estimate LAI of forests in the Järvelja region. The applicability of any of the regression equations obtained to wider areas is a topic for further studies.

### Acknowledgement

*This work has been performed within the VALERI project and supported by the Estonian Science foundation grant no 6815.*

### References

- Ahern, F.J., Erdle, T., Maclean, D.A. and Knepeck, I.D. 1991. A quantitative relationship between forest growth rates and Landsat Thematic Mapper reflectance measurements. *International Journal of Remote Sensing*, 12(3): 387-400.
- Anderson, M.C. 1964. Studies of the woodland light climate. I. The photographic computation of light condition. *Journal of Ecology*, 52: 27-41.
- Brown, L., Chen, J.C., Leblanc, S.G. and Cihlar, J. 2000. A shortwave infrared modification to the simple ratio for LAI retrieval in boreal forests. *Remote Sensing of Environment*, 71: 6-25.
- Cescatti A. 2007. Indirect estimates of canopy gap fraction based on the linear conversion of hemispherical photographs - Methodology and comparison with standard thresholding techniques. *Agricultural and Forest Meteorology* 143(1-2): 1-12.
- Chen, J.M., Pavlic, G., Brown, L., Cihlar, J., Leblanc, S.G., White, H.P., Hall, R.J., Peddle, D.R., King, D.J., Trofymov, J.A., Swift, E., Van der Sanden, J. and Pellikka, P.K.E. 2002. Derivation and validation of Canada-wide coarse-resolution leaf area index maps using high-resolution satellite imagery and ground measurements. *Remote Sensing of Environment*, 80: 65-184.
- Chen, J.M., Rich, P.M., Gower, S.T., Norman, J.M. and Plummer, S. 1997. Leaf area index measurements of boreal forests: Theory, techniques, and measurements. *Journal of Geophysical Research*, 102,D24: 29,429-29,443.
- Chen, J. M. and Leblanc, S. G. 1997. A 4-scale bidirectional reflection model based on canopy architecture. *IEEE Transactions on Geoscience and Remote Sensing*, 35: 1316-1337.
- Evans, G.C. and Coombe, D.E. 1959. Hemispherical and woodland canopy photography and the light climate. *Journal of Ecology*, 47: 123-144.
- Fernandes, R.A., Miller, J.R., Chen, J.M. and Rubinstein, I.G. 2004. Evaluating image-based estimates of leaf area index in boreal conifer stands over a range of scales using high-resolution CASI imagery. *Remote Sensing of Environment*, 89: 200-216.
- Jonckheere, I., Fleck, S., Nackaerts, K., Muys, B., Coppin, P., Weiss, M. and Baret, F. 2004. Review of methods for in situ leaf area index determination Part I. Theories, sensors and hemispherical photography. *Agricultural and Forest Meteorology*, 121: 19-35.
- Kucharik C.J. and Norman J.M. 1996. Measuring canopy architecture with a multiband vegetation Imager (MVI). In: Proc. 22nd conf. on agricultural and forest meteorology, 1996, Atlanta, Georgia. Boston, American Meteorological Society, 128-30.
- Lang, M., Nilson, T., Kuusk, A., Kiviste, A., and Hordo, M. 2007. The performance of foliage mass and crown radius models in forming the input of a forest reflectance model: A test on forest growth sample plots and Landsat 7 ETM+ images. *Remote Sensing of Environment*, 110: 445-457.
- Lükk, T. 1999. Calculation of reflectance in satellite images by means of PixelWin program. *Trans. Faculty Forestry, Estonian Agricult. Univ.*, No 22, p. 88-95 (In Estonian).
- Marklund, L. G. 1988. Biomass functions for pine, spruce and birch in Sweden. Tech. Rep., Swedish University of Agricultural Sciences, Department of Forest Survey, Umeå, Sweden, Vol. 45, p. 73.
- Niinemets, Ü. and Kull, K. 1994. Leaf weight per area and leaf size of 85 Estonian woody species in relation to shade tolerance and light availability. *Forest Ecology and Management* 70: 1-10.
- Nilson, T. 1999. Inversion of gap frequency data in forest stands. *Agricultural and Forest Meteorology*, 98-99: 437-448.
- Nilson, T. and Kuusk, A. 2004. Improved algorithm for estimating canopy indices from gap fraction data in forest canopies. *Agricultural and Forest Meteorology*, 124 (3-4): 157-169.
- Nilson, T., Lükk, T., Suviste, S., Kadarik, H., and Eenmäe, A. 2007. Calibration of time series of satellite

- images to study the seasonal course of forest reflectance. *Proc. Estonian Acad. Sci. Biol. Ecol.*, 56(1): 5-18.
- Orlov, M. M.** 1929. *Forest Taxation*. Leningrad (in Russian).
- Ozolins, R.** 2002. Forest stand assortment structure analysis using mathematical modelling. *Forestry Studies, Estonian Agricultural University*, 37: 33-42.
- Rossello, P.** 2007. Ground data processing & production of the level 1 high resolution maps. [http://www.avignon.inra.fr/valeri/Europe/Estonie/2007/July\\_2007/biomap/JarveljaJuly2007FTReport.pdf](http://www.avignon.inra.fr/valeri/Europe/Estonie/2007/July_2007/biomap/JarveljaJuly2007FTReport.pdf)
- Smolander, H. and Stenberg, P.** 1996. Response of LAI-2000 estimates to changes in plant surface area index in a Scots pine stand. *Tree Physiology*, 16:345-349.
- Stenberg, P., Rautiainen, M., Manninen, T., Voipio, P. and Smolander, H.** 2004. Reduced simple ratio better than NDVI for estimating LAI in Finnish pine and spruce stands. *Silva Fennica*, 38: 3-14.
- Vermote, E.F., Tanrè, D., Deuzé, J.L., Herman, M., and Morcrette, J.J.** 1997. Second simulation of the satellite signal in the solar spectrum, 6S: an overview. *IEEE Transactions in Geoscience and Remote Sensing*, 35: 675-686.
- Watson, D.J.** 1947. Comparative physiological studies in the growth of field crops. I. Variation in net assimilation rate and leaf area between species and varieties, and within and between years. *Annals of Botany*, 11: 41-76.
- <http://modis.gsfc.nasa.gov/> 2008, May, 19.
- <http://www.avignon.inra.fr/valeri/> 2008, May, 19.
- [http://www.avignon.inra.fr/can\\_eye/](http://www.avignon.inra.fr/can_eye/) 2008, May, 19.

Received 16 July 2008  
Accepted 30 October 2008

## ИНДЕКС ЛИСТОВОЙ ПОВЕРХНОСТИ НА ОСНОВЕ ОПТИЧЕСКИХ ИЗМЕРЕНИЙ

А. Кодар, Р. Кутсар, М. Ланг, Т. Люкк, Т. Нильсон

### Резюме

Наземные оценки индекса листовой поверхности (LAI) лесов в Ярвселя, Эстония, получены при помощи наземных измерений анализаторами полого LAI-2000 и путем обработки полусферических фотографий полого, а также используя аллометрические уравнения между традиционными лесотаксационными параметрами и массой листьев. Установлены регрессионные связи между LAI и коэффициентами спектральной яркости, или комбинированными спектральными индексами, определенными с помощью космических снимков мультиспектральных сканеров SPOT и Landsat. Наилучшие корреляции получены между LAI и индексом RSR определенным с помощью красного, ближнего инфракрасного и среднего инфракрасного каналов сканеров. Используя полученные регрессионные связи, стандартное отклонение оценки LAI с космических снимков остается высоким, порядка 1.5 или выше.

**Ключевые слова:** индекс листовой поверхности, лес, дистанционное зондирование.